JOURNAL OF MATERIALS SCIENCE 30 (1995) 2446–2454

The effect of annealing temperature on the fracture performance of isotactic polypropylene

P. M. FRONTINI*, A. FAVE‡
Instituto en Ciencia y Tecnologia de Materiales (INTEMA), UNMDP y CONICET, Juan B. Justo 4302, (7600) Mar del Plata, Argentina

The influence of annealing temperature on the fracture behaviour of a commercial extrusion-grade isotactic polypropylene was studied. Fracture mechanics analysis was carried out at room temperature and at a low crosshead speed under J-controlled conditions. Parameters characterizing fracture initiation, J_{IC}, and crack propagation, T_M, were determined. Some thermal treatments induced "ductile instability" after a certain amount of crack extension while others strongly enhanced the fracture toughness parameters and promoted completely stable behaviour. Aiming to correlate mechanical properties with the supermolecular structure, the different morphologies induced by thermal treatments were studied by differential thermal analysis. In addition, a qualitative fracture surface analysis was carried out by SEM. Craze formation appeared to be the principal plastic deformation mechanism present. The degree of crystallinity and the degree of interconnection related to the thermal treatment the sample had undergone, are the main structural factors controlling fracture performance.

1. Introduction

The mechanical and fracture performance of semicrystalline polymers such as polyolefins appears to be highly influenced by the processing conditions affecting the supermolecular structure. Great efforts have been made towards understanding the role of the crystalline morphology, expressed as tie-chain density, crystallinity, lamellar structure and lamellar thickness, associated to the different thermal histories the material has undergone [1–8]. However, most features of this behaviour remain unsolved.

Isotactic polypropylene has been extensively used in the pipe manufacturing industry owing to its rigidity and thermal stability, but with the disadvantage of being quite brittle at room temperature, and exhibiting poor resistance to crack propagation. In pipe manufacturing, the thermal history applied can be expected to have a great influence upon the final properties of the material.

The purpose of the present studies was to analyse the effect of annealing temperature upon fracture propagation, under static conditions, of an isotactic polypropylene (PP) pipe-grade material.

By annealing PP samples at different temperatures it was possible to induce completely different fracture performances.

Owing to the non-linear characteristics exhibited by PP, the resistance of the material to crack propagation was characterized using the J-integral R-curve approach. The fracture toughness at crack initiation was analysed in terms of the critical fracture initiation parameter, J_{IC}, while the resistance to crack propagation was analysed using the tearing modulus, T_M, concept.

The different morphologies induced by annealing were studied by DSC and fracture surfaces were qualitatively analysed by SEM.

2. Experimental procedure

2.1. Materials

Studies were performed on a commercial extrusion-grade isotactic polypropylene (PP), produced by Petroquimica Cuyo with the trade name of Cuyolem, which has a melt flow index equal to 0.743 g/10 min (ASTM D 11238 L: 2.16 kg at 230 °C). Pellets were compression moulded into plaques at 200 °C and 4.3 MPa and then rapidly cooled down with running water. The plaques were then annealed in an oven for 3 h at temperatures varying between 90 and 160 °C, and then slowly cooled to room temperature in order to avoid the generation of residual thermal stresses.

Henceforth, the annealed samples will be coded with their corresponding annealing temperature, specified after PP.

2.2. Specimen preparation and test conditions

Fracture characterization was carried out on three-point bend specimens (SENB), cut from the compression-moulded plates. Samples were machined to

* Author to whom correspondence should be addressed.
‡ *Present address*: Department Génie Physique Matériaux, INSA de Lyon, France.

0022–2461

reach the final dimensions and improve edge surface finishing.

Preliminary studies were carried out on 10 mm thick (B) conventional specimens, but almost all the results presented herein were made on 8 mm thick (B) side-grooved specimens. The angle of the side grooves was 45° and the thickness was reduced by 20%. Specimens were side-grooved before sharp notching. All the samples were post-mortem remeasured.

Sharp notches were introduced by scalpel-sliding a razor blade having an on-edge tip radius of 13 μm. A crack, a, to depth, W, ratio equal to 0.5 and span to depth ratio equal to 4 were used.

Plaques 4 mm thick were also moulded in order to obtain dumb-bell specimens for yield stress, σ_y, and bars for flexural modulus, E, determination.

All mechanical testing was carried out at 1 mm min^{-1} crosshead rate speed and room temperature.

2.3. Thermal characterization

Differential scanning calorimetry measurements of the moulded specimens were performed in a Du Pont 990 equipment on samples taken from the "brittle fractured zone" (see Section 3.3), whose weights ranged from 4–6 mg. The scanning rate used was 10 °C min^{-1}.

The melting temperature, T_p, was determined at the peak temperatures of the endotherms. The degree of crystallinity was estimated from the measured heat of fusion, assuming an average value for the heat of fusion of 100% crystalline PP equal to 165 J g^{-1} [9].

2.4. Fracture characterization

J-resistance curves were determined by the multiple-specimen technique [10, 11] consisting of loading a series of identical specimens to different amounts of crack extension and then unloading. The value of J for each specimen was determined from the load–displacement curve by the approximate equation proposed by Rice [12]

$$J = \frac{2U}{B(W-a)} \tag{1}$$

where the fracture energy, U, is the area under the load–deflection curve and B, W, and a are the thickness, width and initial notch length, respectively.

The amount of crack extension, Δa, for stable crack propagation was evinced by painting it with an ethyl acetate-based red ink before unloading. The tested samples were completely fractured, after the paint had dried, in a Charpy pendulum at room temperature and Δa determined from the surface, using a 10 × profile projector.

J–R curves were fitted following the procedure recommended by the standard ASTM E813-81. This procedure proposes a linear fitting of the experimental stable crack growth data. The crack initiation value J_{IC}, was defined following the ASTM E813-81 recommendations at the intersection between the theoretical expression for the blunting line

$$J = 2\sigma_y \Delta a \tag{2}$$

and the linear fitted J–R curve. In order to guarantee plane strain conditions at the crack tip, ASTM metal standard recommends working to the following size conditions

$$B, W - a > 25\frac{J_{in}}{\sigma_y} \tag{3}$$

For crack propagation studies, J–R curves were also fitted using exponential J–R approximation (power law fitting)

$$J = C_1 \Delta a^{C_2} \tag{4}$$

where C_1 and C_2 are constants.

The material resistance to crack propagation after J_{IC} was exceeded, was characterized by the tearing modulus

$$T_M = \frac{E}{\sigma_y^2}\frac{dJ}{d\Delta a} \tag{5}$$

which mainly depends on the slope of the J–R curve [13].

2.5. Fractography

Fracture surfaces were examined by SEM using a Jeol JSM 35 CF apparatus, after coating the broken surfaces with a thin gold layer.

3. Results and discussion

3.1. Thermal properties

Representative differential scanning calorimetry (DSC) thermograms of the annealed specimens are illustrated in Fig. 1.

In Table I, the average values of melting points and crystallinity contents are reported as a function of the annealing temperatures. The unannealed samples showed larger dispersion in the values of heat of fusion taken from different points from the same plate and among different plates, probably because of the thermal profiles generated during cooling. A slight increase in crystallinity with annealing temperature was observed.

T_p could be taken as an indication of the lamellar thickness. Except for the sample annealed at 160 °C, which exhibited a definitely higher T_p (163 °C), the melting point was practically uninfluenced by the annealing temperature.

Regarding the shape of the thermograms, some samples (PP-90, PP-120, PP-140, PP-150) exhibited a shoulder. Multiple endotherms have been reported previously for PP [14–16] and have been attributed to two different crystalline forms, crystallites of different size and/or perfection degree. As the annealing temperature was increased peaks became more acute, suggesting an enhancement of crystalline perfection.

3.2. Load–displacement curves

Typical load–displacement curves of the specimens for different annealed treatments are shown in Fig. 2. All

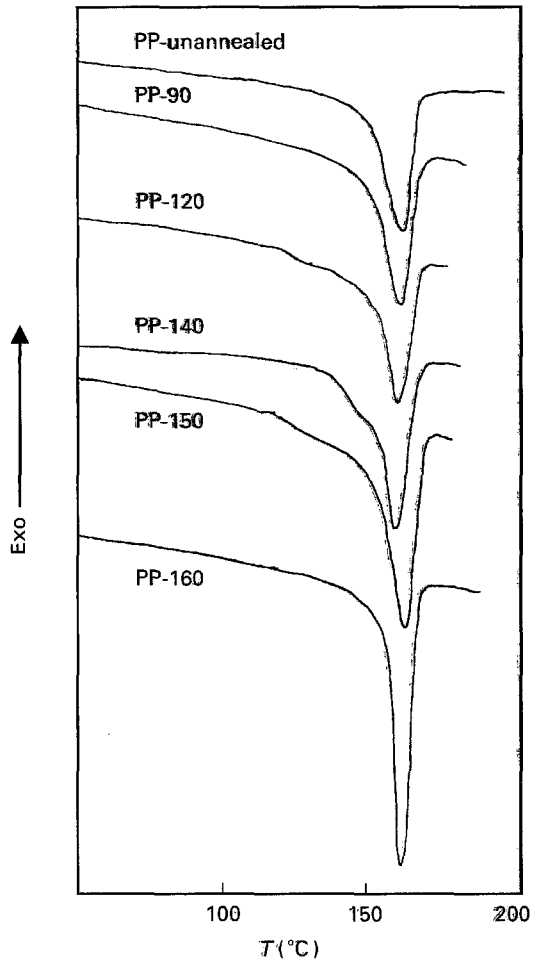

Figure 1 Thermograms of unannealed and annealed PP samples.

TABLE I Thermal properties of the PP samples unannealed and annealed at different temperatures

Sample	Annealing temperature (°C)	Crystallinity (%)	Melting temperature (°C)
PP-unannealed	–	53.9	161.0
PP-90	90	59.4	161.3
PP-120	120	60.4	161.6
PP-140	140	63.6	161.7
PP-150	150	63.0	161.7
PP-160	160	66.0	163

of them exhibited a great deviation from linearity, arising from the growth of a significant damage zone at the crack tip ("stress-whitening") as well as from the initiation of subcritical growth before the maximum load. Two types of behaviour were found.

(a) Stable–unstable: In some cases, at a certain deflection after the maximum load (PP-as-moulded, PP-90 and PP-120), and at a certain amount of stable propagation (as it emerged from the fracture surface inspection), sudden instability occurred and the specimen broke in two halves which literally flew away aided by the energy provided by the elastic strain energy stored in the sample. This phenomenon is called "ductile instability".

(b) Completely stable: In the other cases (PP-140, PP-150, PP-160), completely stable fracture was

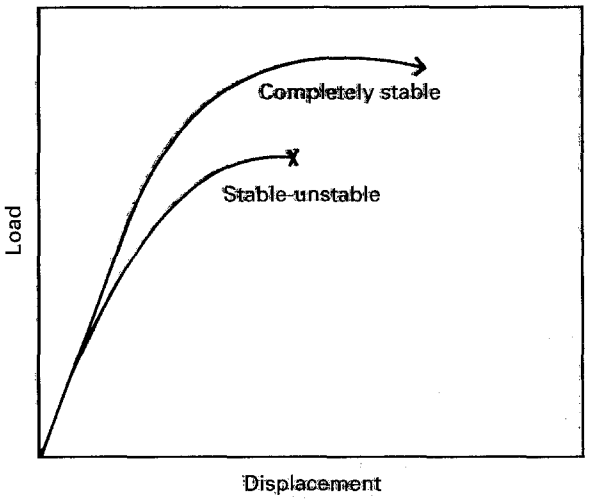

Figure 2 Load–displacement curves of the two typical types of behaviour displayed by the samples.

observed, the crack grew with the continuous supply of energy from the external load and with continuous increase in displacement until complete fracture.

Owing to the non-linearity exhibited by load–displacement curves, linear elastic fracture mechanics is not applicable in any of these two cases.

This stable–unstable transition regime under displacement control conditions for depth-notched specimen behaviour in PP was detected previously by other authors [17–19].

A complementary experiment was carried out to confirm this observation. A PP-90 sample, which first exhibited the "ductile instability" phenomenon, was reannealed for 3 h at 150 °C. Then, a normal fracture test was performed. This time the sample exhibited a completely stable behaviour, thus, confirming that it is possible to erase the effect induced by thermal treatment below 120 °C on isotactic polypropylene by submitting the sample to an adequate thermal treatment.

3.3. Fractographic analysis

Fig. 3a and b show typical macrophotographs of the fracture surface of a pendulum-broken sample after some stable crack growth had occurred for a conventional specimen and for a side-grooved one. In both photographs a clear demarcation between the subcritical growth region and the brittle region can be seen. Fracture has developed from the initial razor notch followed by some amount of stable crack growth. It is possible also to appreciate a white halo corresponding to the crazed zone, developed at the crack tip prior to crack advance, and the differences in roughness between the stable crack growth and the crazed regions. In the centre of the specimen the crack and the whitened halo had propagated further ahead than at the edges of the crack front indicating the more critical three-dimensional stress state generated in the interior of the material. In the case of side-grooved specimens, a straighter crack is observed due to the additional constraint generated at the edges.

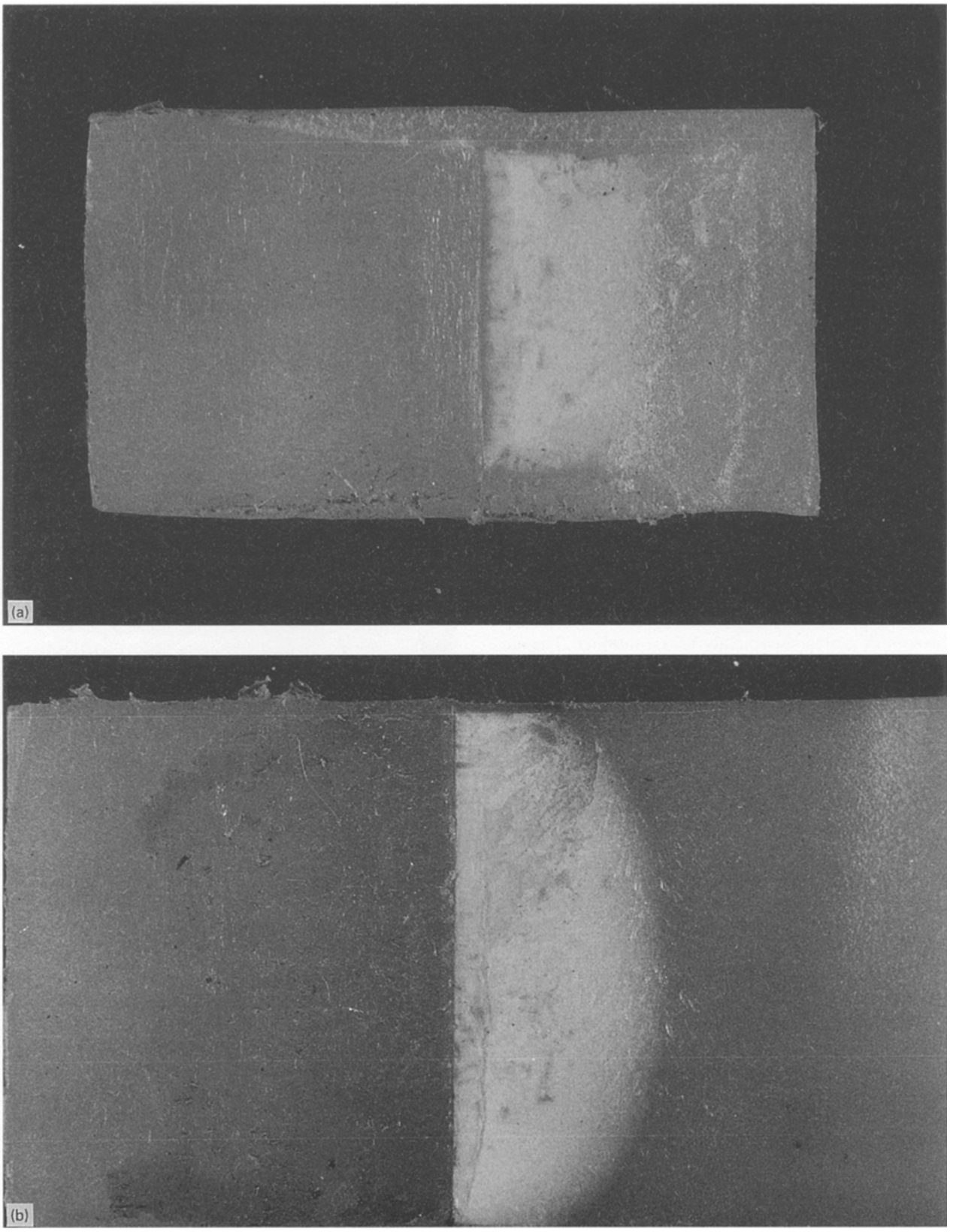

Figure 3 Photographs of the fractured surfaces of (a) a conventional specimen, and (b) a side-grooved specimen.

Fig. 4 shows a magnification of the surface of a PP-120 sample propagated up to the instability point. In the micrograph the fracture nucleus is clearly seen where the instability had generated.

Figs 5 and 6 show a series of micrographs of the fracture surfaces of PP-90 and PP-160 samples, respectively. These samples exhibited a completely different phenomenological behaviour. PP-160 always broke in a stable manner, while PP-90 broke stable–unstably. For the PP-90 series, Fig. 5a shows a general view of the surface. Three distinct patterns can be distinguished: the smooth razor-blade notch region, the stable crack propagation zone, and the unstable brittle fracture. Fig. 5b is a higher magnification

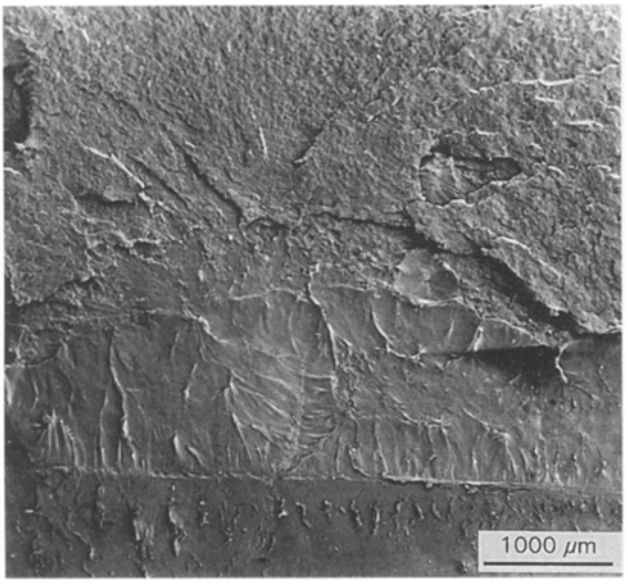

Figure 4 A micrograph of the fractured surface of a PP-120 sample. The crack propagated from the bottom.

of the stable crack propagation zone. The material appears oriented in the crack propagation direction displaying macroductile type of failure. Fig. 5c shows a higher magnification of the stress-whitened zone, broken in a macroscopically brittle manner. The surface does not appear drawn as in Fig. 5b, but still has clear evidence of microductility on the fracture surface. This kind of fracture surface, showing microductile zones (whiteness) and voids, was called "quasi-cleavage" fracture type [20].

For the PP-160 series, Fig. 6a shows a general view of the surface of the PP-160 sample and also three distinct surface patterns can be distinguished: the smooth razor-blade notch region, the stable crack propagation zone, and the brittle Charpy broken surface. Fig. 6b shows a magnified view of the stable crack propagation zone region; failure is clearly seen to have occurred by viscous tearing, typical of a J-controlled fracture, consistent with the macroscopic behaviour observed. The surface shown in Fig. 6c is very similar to the analogous one in PP-90, and corresponds to the crazed damaged zone which preceded the crack brittle pendulum fracture had occurred through.

3.4. Mechanical properties

The results for the mechanical properties, σ_y and E, are shown in Table II.

Consistent with expectations, the yield stress exhibited a very slight dependence on the thermal treatment even if a very small increase trend was verified. For the elastic modulus, however, the samples annealed at temperatures above 140 °C exhibited definitely higher values due to the reinforcing action of the crystallites.

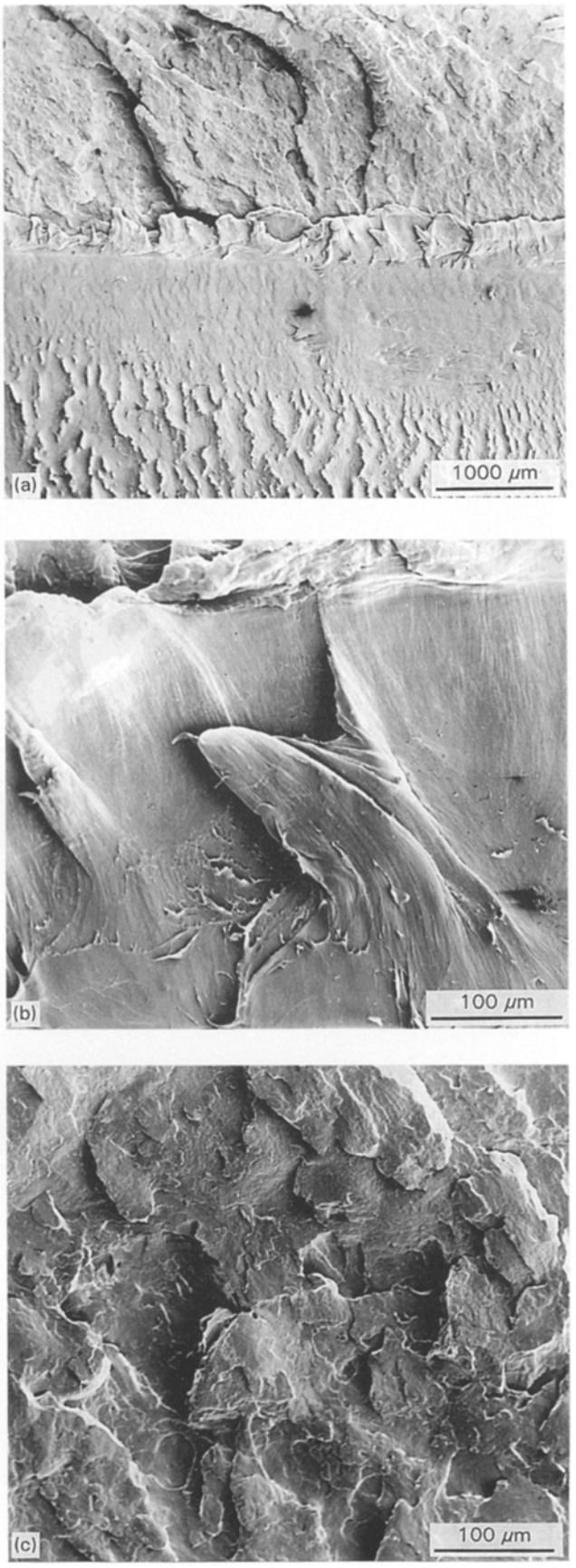

Figure 5 Micrographs showing (a) a general view of a PP-90 fractured sample (the crack propagated from the bottom), (b) the stable crack growth zone, and (c) the brittle fracture zone.

3.5. Crack growth resistance curve (R-curve) and mechanical properties

Fig. 7 shows the resistance curve for PP-as-moulded and the annealed polypropylene samples. Fig. 7a shows part of the preliminary results obtained with conventional and side-grooved specimens for the unannealed PP. This material exhibited stable–unstable behaviour. It showed relatively large data dispersion,

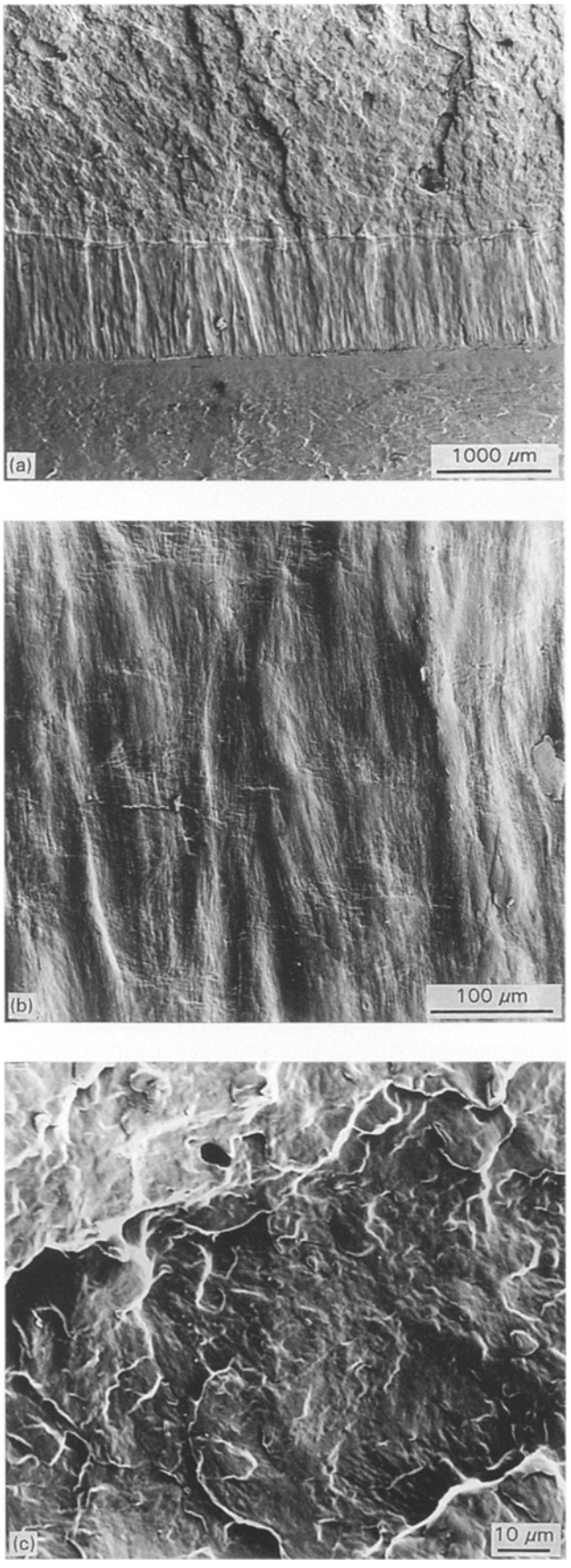

Figure 6 Micrographs showing (a) a general view of a PP-160 fractured sample (the crack propagated from the bottom), (b) the stable crack growth zone, and (c) the Charpy broken zone.

arising from the thermal profiles generating during cooling in the moulding processing, which induces residual stresses. In fact, the largest differences in the heat of fusion for samples taken from different points in one plaque was also verified for this material. For this set of samples, numerical results should be taken with care, even if a fit was attempted.

The straighter crack growth promoted by side-grooving together with the homogeneity promoted by annealing really improved the Δa readings. This is reflected in a reduction of the scatter displayed by the series of samples shown herein (Fig. 7) with respect to the preliminary results. It is worth mentioning that the construction of J–R curves for materials exhibiting ductile instability is not easy and could lead to erroneous conclusions. Many data had to be rejected because, when the samples had reached the prior to stopping the test, painting the surface with red ink was impossible. Under such circumstances, the direct reading of crack growth from the unpainted surface was not always possible. In addition, data points also fell very close to each other, because the advance of the crack was limited to the instability condition. For these cases, an unusually large number of samples was tested to obtain reliable J–R curves.

Even if we worked very close to the limit size requirements (Equation 4), varying in this work between 7 and 13 mm, the experiments shown in Fig. 7e demonstrated that our results have practically no influence on the thickness effects. Conventional 10 mm specimens were tested and the results plotted together with data obtained using side-grooved specimens: all the data scattered in the same dispersion band, thus confirming that our results are still comparable.

J_{IC} values are shown in Table II: an increasing trend in the initiation to fracture values with increasing crystallinity was found. In every case, all the initiation values were relatively high, and consistent with K and J values published previously [21, 22] for PP. However, the more relevant fact displayed by this material (the abrupt change in crack propagation regime from stable–unstable to completely stable) is obviously not reflected in J_{IC} which appears incomplete in describing the whole fracture behaviour.

Paris *et al.* [13] developed a theory to explain the crack instability phenomenon in terms of J-integral R-curves in order to study instability in metals under J-controlled conditions. They stated that sudden instability occurs when an applied situation, depending on loading systems and geometry, exceeds the tearing modulus of the material (Equation 5). This parameter, T_M, describes the material's ability to resist crack propagation after J_{IC} is exceeded, and it mainly depends on the slope of the J–R curve.

In a recent paper, Hashemi and Williams [22] successfully applied the tearing modulus criterion to predict the stable behaviour of their materials using the simplest expression proposed by Paris *et al.* for the applied tearing modulus, T_{app}, corresponding to a complete displacement control situation and fully plastic conditions

$$T_{app} = \frac{2(W - a)^2}{W^3} \tag{6}$$

TABLE II Mechanical properties of the PP samples unannealed and annealed at different temperatures

Sample	J_{IC} (N mm^{-1})	σ_y (MPa)	E (GPa)	Crystallinity (%)	T_M
PP-unannealed	11.9	28	1.4	53.9	29.0
PP-90	9.4	31.5	1.45	59.4	24.0
PP-120	12.3	32.3	1.45	60.4	18.0
PP-140	15.8	32.6	1.5	63.6	37.0
PP-150	17.2	33.0	1.66	63.0	36.5
PP-160	17.4	33.3	1.74	66.0	48.6

equal to 2 at the onset of the test. If we apply this criterion to our materials using the slope of the linear regression as they did, we also would predict, but erroneously, stable behaviour during all the tests.

However, Narisawa and Takemori [23] previously attempted to apply this criterion to polymers without success. They were not able to observe plastic collapse of the remaining ligament in their samples, and explained their results basically by the presence of crazing and cavitation at the crack tip. The calculation of T_{app}, assuming incomplete fully plastic conditions, is not very simple. This seems also to be the case of our materials which mainly deformed by crazing.

However, without pretending to predict the instability, the tearing modulus could still be used to describe qualitatively the differences in crack propagation.

Table II also shows the calculated values of T_M from the slope of linear fitted J–R curves. It seems that materials exhibiting completely stable behaviour have a higher T_M even if no clear trend was found.

Paris *et al.* also pointed out [13] that many experimentally determined R-curves appear to be curved downwards as tearing progresses extensively. That implies, at least in some cases, that dJ/da may diminish with crack extension very quickly instead of having a constant value throughout the test. This can be observed in Fig. 8 for samples exhibiting stable–unstable behaviour. In this figure, all the power-law fitted curves (Equation 4, Fig. 8a) for the annealed samples and the corresponding dJ/da calculated from the fitted expressions (Fig. 8b), were plotted together to make the differences relevant in curve shapes and the maximum J-values that each PP material can reach.

3.6. Annealing effect upon fracture propagation mode

From the results shown above, it seems that annealing temperatures below 120 °C act only as stress relievers having practically no influence upon fracture propagation. Annealing temperatures above the crystallization temperatures, however, do improve the whole crack propagation behaviour. The change in the propagation mode appears to be related to an increase in crystallinity promoted by treatments above the crystallization temperature (close to 135 °C) while the fracture initiation value seems to be more related to the degree of crystal perfection induced by annealing close to the melting point, i.e. 150 and 160 °C.

Other authors have previously denounced the improvement in fracture behaviour by annealing in PP, even if they studied different features of this phenomenon [2, 6].

Varga [14], in his excellent review, explained that spherulite boundaries act at "weak sites", and failure often initiated on these spots by coalescence of microvoids and crazes. The weakness of this zone arose from the non-crystallizing component which is accumulated in these regions. Hornbogen and Friedrich [24] proved that cracks propagate easily at the interfaces between coarse spherulites and that fracture can be improved by improving intercrystalline and interspherulitic links.

Vu-Khanh and Fisa [18] stated that in PP, void coalescence is responsible for unstable fracture, and promoting matrix drawing and stretching is possible to prevent the coalescence of voids which normally occurs in the craze region of PP, causing catastrophic failure. Moreover, in other plastics, the sudden instability [25, 26] has been explained as a consequence of the transition from multiple to single crazing.

Consistent with Spahr *et al.'s* [26] findings, the surface morphology of the stable part of crack growth of the materials studied here, exhibited greater plastic deformation. The greater the ability to undergo plastic deformation the more stable crack propagation will be. It appears that this ability in PP is obviously associated with the annealing temperature. Annealing at temperatures close to the melting point prevents the coalescence of voids and crazes, allowing for more plastic deformation at the matrix.

On the other hand, Greco pointed out [2] that annealing operates through partial melting and recrystallization processes which lead to the growth of thin crystallites and a rearrangement of uncrystallized polymer chains mainly in the interspherulitic zones. These explanations seem to be consistent with the results shown in this paper. This more interconnected physical network resulting from thermal annealing, appears to impede the craze coalescence and allow larger plastic deformation.

4. Conclusions

The influence of thermal annealing upon J-controlled crack propagation performance has been analysed. Annealing temperatures below 120 °C promote only residual thermal stress relaxations, while annealing at higher temperatures always induces stable crack propagation.

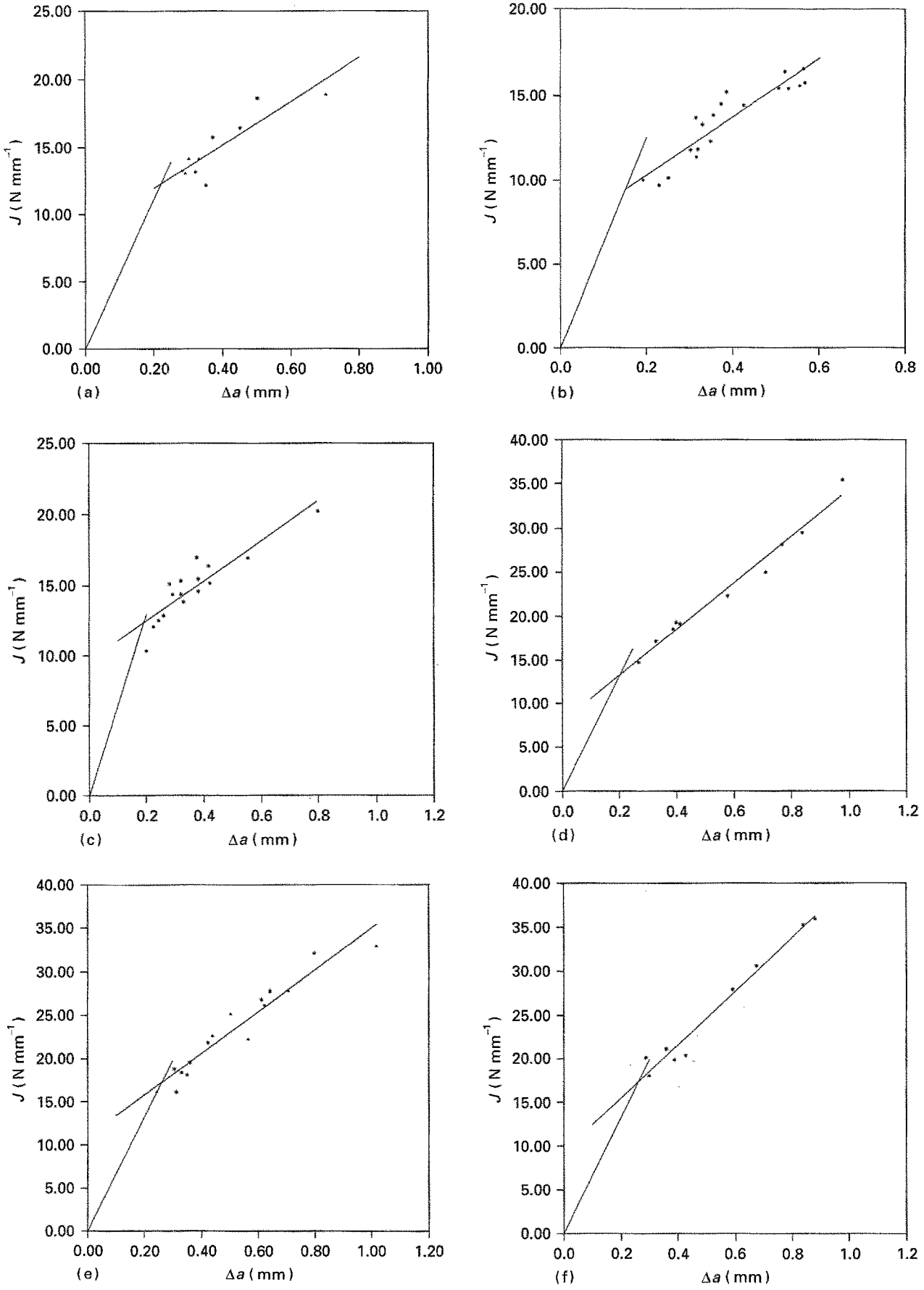

Figure 7 J-values versus crack growth for the different samples: (a) PP-unannealed, (*) side-grooved, (▲) conventional; (b) PP-90; (c) PP-120; (d) PP-140; (e) PP-150, (*) side-grooved, (▲) conventional; (f) PP-160.

Annealing above 140 °C enhances crystallinity of the molecular superstructure mainly in the inter-spherulitic zones, which prevents craze and void coalescence. Only at temperatures very close to the melting point (160 °C) does annealing have a practical influence on T_p.

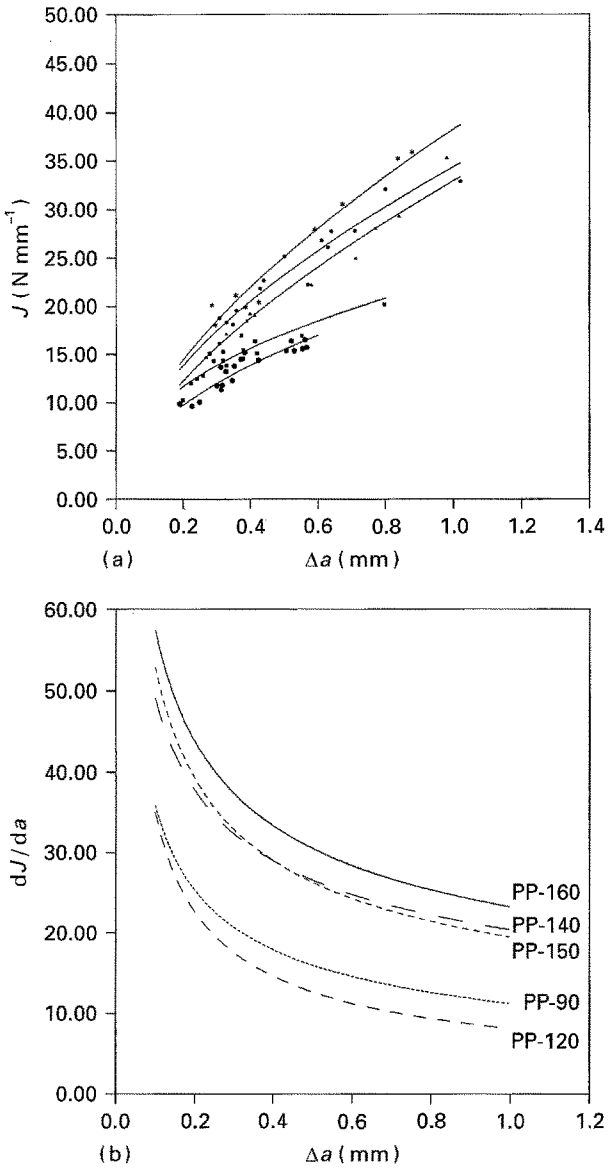

Figure 8 (a) Power law J–R resistance curve for unannealed and annealed samples: (*) PP-160, (●) PP-150, (▲) PP-140, (■) PP-120, (●) PP-90. (b) The slope of the power law J–R resistance curve for unannealed and annealed samples plotted against crack extension.

An increasing trend of the critical initiation to fracture value with crystallinity was found.

The entire fracture behaviour can be qualitatively analysed by comparing the J–R curves or by means of tearing modulus analysis, even if an actual criterion capable of predicting the instability has not been considered.

From the above discussion it becomes clear that the main finding of this work is the transition regime in the crack propagation behaviour (from stable–unstable to completely stable) promoted by annealing temperatures above 140 °C. This result has an important implication in the safety design of structural parts made of PP.

Acknowledgement

The authors thank Petroquímica Cuyo for supplying materials.

References

1. J. RUNT and M. JACQ , *J. Mater. Sci.* **24** (1989) 1421.
2. R. GRECO and G. RAGOSTA, *ibid.* **23** (1988) 4171.
3. M. R. BRAGA, M. RINK and A. PAVAN, *Polymer* **32** (1991) 3152.
4. A. O. BARANOV and E. V. PRUT, *J. Appl. Polym. Sci.* **44** (1992) 1557.
5. M. A. KAY, *Br. Polym. J.* **21** (1989) 285.
6. J. I. ITO, K. MITANI and Y. MIZUTANI, *Jpn Appl. Phys. Soc.* **46** (1992) 1221.
7. Y. L. HUANG and N. B. NITO, *J. Polym. Sci. B Polym. Phys.* **29** (1991) 129.
8. R. SEGUELA and F. RIETSCH, *Polymer* **27** (1986) 532.
9. B. WUNDERLICH, "Macromolecular Physics" Vol. 3 (Academic Press, New York, 1980) p. 63.
10. S. HASHEMI and J. G. WILLIAMS, *Polym. Eng. Sci.* **26** (1986) 760.
11. C. R. BERNAL, P. M. FRONTINI and R. HERRERA, *Polym. Test.* **11** (1992) 271.
12. J. R. RICE, *J. Appl. Mech.* **35** (1968) 379.
13. P. C. PARIS, H. TADA, A. ZAHOOR and H. ERNST, "Elastic Plastic Fracture", ASTM STP 668 (American Society for Testing and Materials, Philadelphia, PA, (1979) p. 5.
14. J. VARGA, *J. Mater. Sci.* **27** (1992) 2557.
15. W. F. MSUYA and C. YUE, *J. Mater. Sci. Lett.* **8** (1989) 1266.
16. Y. S. YADAV and P. C. JAIN, *Polymer* **27** (1986) 721.
17. T. VU-KHANH, B. SANCHARUIN and B. FISA, *Polym. Compos.* **6** (1985) 249.
18. T. VU-KHANH and B. FISA, *Theor. Appl. Fract. Mech.* **13** (1990) 11.
19. I. NARISAWA, *Polym. Eng. Sci.* **27** (1987) 41.
20. S. F. XAVIER, J. M. SCHUTZ and K. FRIEDRICH, *J. Mater. Sci.* **25** (1990) 2411.
21. J. G. WILLIAMS, "Fracture Mechanics of Polymers" (Ellis Horwood, London, 1984) p. 173.
22. S. HASHEMI and J. G. WILLIAMS, *J. Mater. Sci.* **26** (1991) 621.
23. I. NARISAWA and TAKEMORI, *Polym. Eng. Sci.* **28** (1988) 1462.
24. E. HORNBOGEN and K. FRIEDRICH, *J. Mater. Sci.* **15** (1980) 2175.
25. L. H. LEE, J. F. MANDEL and F. J. Mc GARRY, *Polym. Eng. Sci.* **27** (1987) 1128.
26. D. E. SPAHR, K. FRIEDRICH, J. M. SCHULTZ and R. S. BAILEY, *J. Mater. Sci.* **25** (1990) 4427.

Received 26 May 1993
and accepted 10 October 1994